

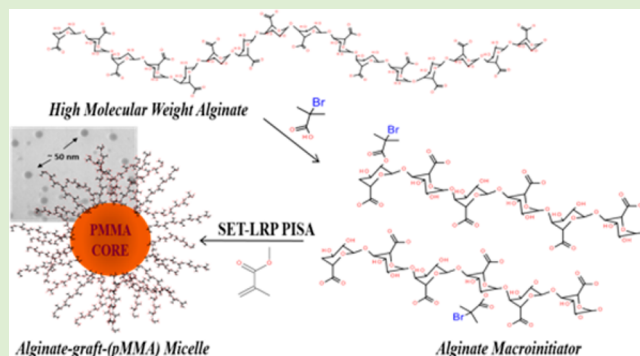
Polymerization Induced Self-Assembly of Alginate Based Amphiphilic Graft Copolymers Synthesized by Single Electron Transfer Living Radical Polymerization

Vitaliy Kapishon,[†] Ralph A. Whitney,[‡] Pascale Champagne,^{†,§} Michael F. Cunningham,^{*,†,‡} and Ronald J. Neufeld^{*,†}

[†]Department of Chemical Engineering, [‡]Department of Chemistry, and [§]Department of Civil Engineering, Queen's University, Kingston, Ontario Canada K7L 3N6

S Supporting Information

ABSTRACT: Alginate-based amphiphilic graft copolymers were synthesized by single electron transfer living radical polymerization (SET-LRP), forming stable micelles during polymerization induced self-assembly (PISA). First, alginate macroinitiator was prepared by partial depolymerization of native alginate, solubility modification and attachment of initiator. Depolymerized low molecular weight alginate (~12 000 g/mol) was modified with tetrabutylammonium, enabling miscibility in anhydrous organic solvents, followed by initiator attachment via esterification yielding a macroinitiator with a degree of substitution of 0.02, or 1–2 initiator groups per alginate chain. Then, methyl methacrylate was polymerized from the alginate macroinitiator in mixtures of water and methanol, forming poly(methyl methacrylate) grafts, prior to self-assembly, of ~75 000 g/mol and polydispersity of 1.2. PISA of the amphiphilic graft-copolymer resulted in the formation of micelles with diameters of 50–300 nm characterized by light scattering and electron microscopy. As the first reported case of LRP from alginate, this work introduces a synthetic route to a preparation of alginate-based hybrid polymers with a precise macromolecular architecture and desired functionalities. The intended application is the preparation of micelles for drug delivery; however, LRP from alginate can also be applied in the field of biomaterials to the improvement of alginate-based hydrogel systems such as nano- and microhydrogel particles, islet encapsulation materials, hydrogel implants, and topical applications. Such modified alginates can also improve the function and application of native alginates in food and agricultural applications.



INTRODUCTION

Natural polymers such as polysaccharides are used in biomedical applications that include implants, tissue engineering and controlled drug delivery because most are considered biocompatible, nontoxic and nonimmunogenic. More specifically, polysaccharide-based micelles have been explored as replacements to fully synthetic polymers for drug delivery.¹ Polysaccharide based amphiphilic materials capable of self-assembly into micelles, are prepared by grafting/conjugating hydrophobic moieties onto the polysaccharide backbone. Such chemical modifications are achieved via utilization of a number of reactive groups, including hydroxyl, amino and carboxyl groups, depending on the polysaccharide.²

The rationale behind using alginate as a drug-delivery carrier is that it has been widely used as a biomaterial and has proven to be biocompatible in various formulations.³ Alginate is a low cost, widely available polyelectrolytic polysaccharide isolated from natural sources as a water-soluble copolymer of mannuronic (M) and guluronic acid (G), arranged irregularly in blocks to form MM, GM/MG, and GG regions.⁴

Mannuronic acid is connected via linear and flexible β (1–4) linkages, whereas guluronic acid is bonded via α (1–4) linkages that reduce molecular flexibility and introduce rigidity.⁵ Both blocks carry a carboxylic acid group, which can be in a neutral or ionized state providing pH-responsive properties. For this reason, alginate is commonly used as a hydrogel, prepared by ionic cross-linking with divalent cations such as calcium.^{3,5–8} Alginate, in its natural form, is a widely used material for biomedical applications due to its unique gelation properties and biocompatibility.⁹ Such applications include encapsulation of cells,¹⁰ enzymes,^{11,12} biopharmaceuticals, and therapeutics.^{13–17} Alginate gel particles are poor small molecule drug carriers due to hydrogel swelling and fast diffusion of the drug, resulting in poorly controlled drug release.¹⁸ Alginate can be chemically modified by reactions of the hydroxyl or carboxyl moieties. Types of modifications include covalent cross-linking,

Received: April 9, 2015

Revised: June 12, 2015

Published: June 12, 2015



oxidation of alginate backbone, attachment of small functional groups or other polymers via esterification, amidation and acetylation, or growing polymers from the alginate backbone.^{19,20} Compared to other polysaccharides such as cellulose, dextran, or starch, chemical modification of alginate has not been widely studied, possibly due to solubility limitations in organic solvents. This is especially true when it comes to grafting hydrophobic polymers from polysaccharides.

Living radical polymerization (LRP), also known as controlled radical polymerization, has been steadily finding its way from academic research into numerous high-value polymer markets due to some key advantages over conventional free radical polymerization.²¹ The advantages include a more precise control over molecular weight, decreased polydispersity and preservation of chain end functionality, allowing for synthesis of complex architectures such as diblock, triblock and star polymers.^{22,23} The primary difference from free radical polymerization and the main principle of LRP is that a growing chain end can be reversibly deactivated by a molecule or atom “capping agent” and subsequently activated by removing the “capping agent”. In the case of atom transfer radical polymerization, the capping agent is usually a bromine or chlorine atom that keeps the propagating chain in a dormant state until it is removed by a catalyst in its lower oxidation state. Single electron transfer living radical polymerization, SET-LRP, also known as activator and reducing agent atom transfer radical polymerization (SARA ATRP),^{22,24} uses small amounts of Cu(0) together with ligand as the catalyst.^{22,24} In SET-LRP catalytic cycle, Cu(0) activates the polymer living end forming Cu(I)X/Ligand complex, initiating propagation. Cu(I)X disproportionates into Cu(0) and Cu(II)X₂ thus regenerating Cu(0). Cu(II)X₂ deactivates the propagating polymer sending it back to the dormant state. SET-LRP has been discovered and meticulously studied by Percec and co-workers^{25–35} polymerizing a number of acrylic monomers in organic solvents, water, and binary organic/water mixtures.

Although there have been no reports to date on the grafting of polymers from alginate using LRP, other polysaccharides, such as cellulose, chitosan, dextran, and galactoglucomannan, have been grafted with polymers using this method. Hiltunen et al.³⁶ reported copolymerization of acrylamide and *N,N*-dimethylacrylamide from cellulose via SET-LRP. Bromoisobutyryl bromide was first reacted with cellulose to produce a macroinitiator (cellulose-Br) with a degree of substitution (DS) of 0.3–2.6. Polymerization was then performed in dimethyl sulfoxide (DMSO) at 80 °C using CuCl as catalyst. Number-average molecular weight (M_n) of the copolymer grafts was 2800–3000 g/mol with polydispersity index (PDI) of 1.1–1.2. The grafted cellulose was then shown to self-assemble in water generating micelles with diameters between 119 and 160 nm. Voepel and co-workers³⁷ functionalized acetylated galactoglucomannan with bromoisobutyryl (BrIB) initiator via 1,1'-carbonyldiimidazole (CDI) activated esterification of hydroxyl groups with bromoisobutyric acid. From this macroinitiator, methyl methacrylate was polymerized using C(0)C-LRP in DMSO, while *N*-isopropylacrylamide and acrylamide were grafted in water. Macroinitiator with molecular weight of 3500 g/mol was used to produce the polymer grafts with molecular weight up to 113 000 g/mol. In other work,³⁸ the same group polymerized methyl acrylate from acetylated galactoglucomannan to generate polymethyl acrylate chains between 4300 and 263 000 g/mol in DMSO, DMF, and DMSO/water.

In this work, we are presenting the first report of living radical polymerization from alginate. This was achieved by preparing low molecular weight alginate via radical degradation using hydrogen peroxide as previously reported by Li et al.³⁹ Low molecular weight alginate was necessary to generate nanoscale micelles. The attachment of the LRP initiator onto the alginate backbone was then performed via esterification of alginate hydroxyl groups. To achieve anhydrous conditions required for esterification, alginate-tetrabutylammonium (TBA) salt was prepared by the protocol described by Pawar and Edgar⁴⁰ to improve alginate solubility in organic solvents. A cosolvent mixture was then developed enabling miscibility of water-soluble macroinitiator and water insoluble monomer. Chain extension via SET-LRP enabled self-assembly as a result of the increasing insolubility of the hydrophobic grafts as polymerization progressed. This is also known as polymerization induced self-assembly (PISA).^{41–43} The advantages of particle preparation by PISA compared to amphiphilic copolymer synthesis in a cosolvent include the ability to conduct polymerizations at higher concentrations, and the elimination of a separate postpolymerization preparation step for self-assembly. Both advantages result in a more efficient process with reduced solvent consumption.

Alginate based amphiphilic materials capable of self-assembly into micelles have been previously synthesized by attaching hydrophobic alkyl groups to alginate backbone. Kang and co-workers⁴⁴ achieved this by first oxidizing alginate with periodate which generated reactive aldehydes and then reacting it with amino terminated short linear alkyl chains (C8, C12, and C16) via reductive amination with help of a reducing agent. Resultant alkyl-grafted alginates self-assembled into micelles with 223 nm in diameter and critical micelle concentration (CMC) of 1.35 g/L. Yang et al.⁴⁵ prepared similar surfactants via aqueous carbodiimide activated esterification of C8, C12, and C16 alkyl alcohols with alginate carboxylic groups. The micelle size ranged between 200 and 600 nm, with the longest alkyl chains producing smallest micelle size, and a CMC of 0.002–0.003 g/L. In the present study, we made an improvement in the design of alginate based micelles by grafting longer chains from alginate via LRP which resulted in reduction of the micelle size, increased hydrophobicity of the core, and having potentially complex multifunctional composition of the micelle core.

Micelles containing alginate as the outer-shell with preserved carboxylate moieties have significant potential in controlled and targeted delivery of therapeutics. One of the benefits is the ability to cross-link the micelles to generate more complex structures. Another is pre- and/or postpolymerization decoration of the alginate backbone to carry bioactive molecules such as drugs⁴⁶ and ligands.⁴⁷

MATERIALS AND METHODS

Materials. Alginic acid sodium salt, from brown algae, viscosity of 2% solution at 25 °C ~ 250 cps M/G ratio of ~1.56, molecular weight 280 000 g/mol (determined by aq-GPC) CAS 9005-38-3 batch# 106 K0113, hydrogen peroxide 30% in water, hydrogen peroxide 50% in water, tetrabutylammonium hydroxide (TBAOH) solution 40% (1.M) in water, tetrabutylammonium fluoride (TBAF) hydrate 98%, tetrabutylammonium fluoride (TBAF) 1.0 M in THF, α -bromoisobutyric acid (BrIBA) ≥98.0% (GC), 1,1'-carbonyldiimidazole (CDI) ≥98.0% (T), dimethyl sulfoxide (DMSO) anhydrous ≥99.9%, *N,N*-dimethylformamide (DMF) anhydrous 99.8%, methyl methacrylate (MMA) ≤99% ppm MEHQ as inhibitor, 99%, tris[2-(dimethylamino)ethyl]amine (Me₆TREN) 97%, copper wire diameter

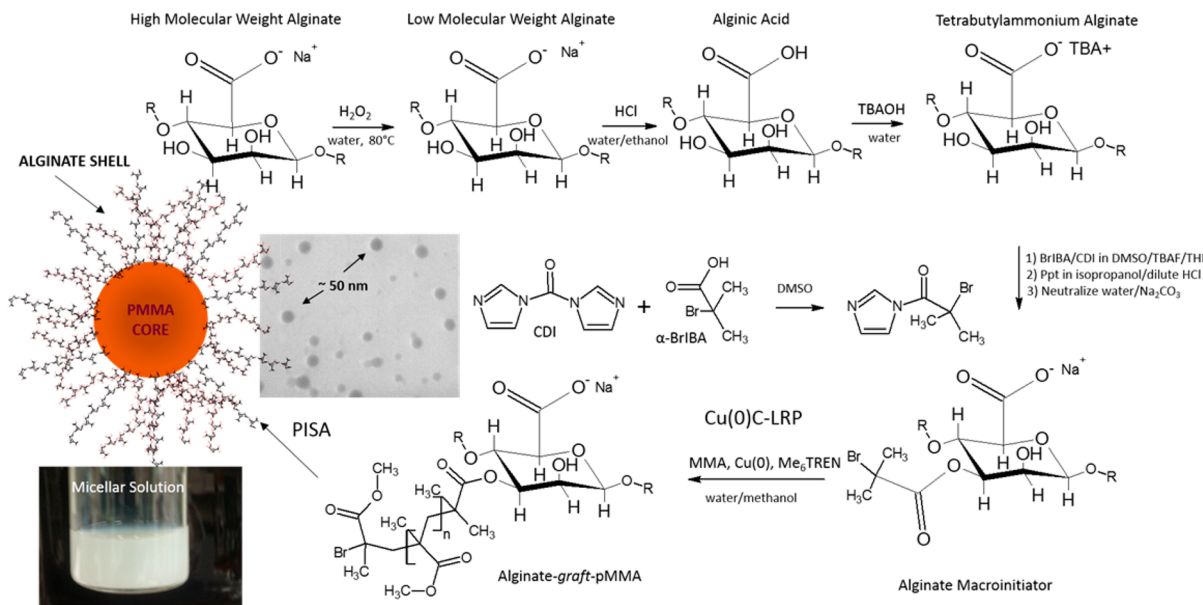


Figure 1. Summary of synthetic route for preparation of alginate-*graft*-pMMA micelles via SET-LRP PISA. Note: structure of macroinitiator shows one of four possible ways BrIBA could be esterified onto alginate backbone: axial and equatorial of mannuronic acid and axial and equatorial guluronic acid (G) which is confirmed by NMR (Figure 4).

1.0 mm ≥99.9%, Coumarin 153 (C153), and dye content 99% were purchased from Sigma-Aldrich.

Characterization. ¹H NMR of all products in D₂O, CDCl₃, or DMSO-*d*₆ was acquired with a Bruker Avance 400 MHz instrument. The molecular weight of alginate was determined with a Viscotek GPCmax 2001 + Viscotek TDA (RI+VISC+RALS) apparatus; mobile phase: 0.05 M sodium nitrate with 0.02% sodium azide in water, calibrated with poly(ethylene oxide) standards. Molecular weight of grafts was analyzed by using a Viscotek 270max instrument with a dual detector; mobile phase: THF. Micelle morphology was observed using a Hitachi H-7000 transmission electron microscope (TEM) (75 kV), calibrated with poly(methyl methacrylate) standards. Micelle size distribution was measured by dynamic light scattering (DLS) at 25 °C using a Malvern Zetasizer Nano Series (Nano ZS). CMC of micelles was determined using a Photon Technology International (PTI) spectrofluorometer with a ThermoNESLAB EX7 bath, PTI Motor Driver MD-5020, PTI shutter controller SC-500, PTI lamp power supply LPS-220B, and PTI 814 photomultiplier detection systems.

Alginate Degradation. In a typical degradation procedure, 7.5 g of high molecular weight alginate was dissolved in 500 mL of distilled water (1.5% w/v), then 3.5 g of ascorbic acid and 5 mL of pyridine were added and the solution placed in an oil bath, bubbled with nitrogen, and heated to 80 °C. Once heated, 50 mL of 30% hydrogen peroxide were added to start the degradation. Samples were withdrawn over time, precipitated with cold ethanol, washed with methanol and lyophilized from water. The final product, low molecular weight alginate was precipitated, washed and lyophilized as in the kinetic study. Degraded alginate was analyzed by dynamic light scattering (DLS) and aqueous gel permeation chromatography (aq-GPC).

Alginate Solubility Modification. Dry low molecular weight alginate (1 g) was added to a 100 mL solution of ethanol/0.6 M HCl in water (1:1 v/v) and stirred overnight at 4 °C. The product was vacuum filtered, washed with ethanol (three times) and acetone (three times), and then dried under vacuum to produce low molecular weight alginic acid. Dry low molecular weight alginic acid was redissolved in water (3% w/v), placed under constant stirring with a pH probe immersed, and then a dilute solution (4% w/v) of tetrabutylammonium hydroxide (TBAOH) was added dropwise until a pH of 7–9 was reached. The resulting solution of low molecular weight alginate-TBA was lyophilized and its solubility tested in DMSO, DMF and THF, each with and without 1% tetrabutylammonium fluoride (TBAF).

Attachment of Initiator. One gram of 1,1'-carbonyldiimidazole (CDI) (6 mmol) and 1 g of α-bromoisoctyric acid (BrIBA) (6 mmol) were dissolved in 10 mL of DMSO in a round-bottom flask and left to react for 1 h under nitrogen at room temperature. In a separate flask, 1 g of alginate-TBA (6 mmol alginate) was dissolved in 30 mL DMSO containing 2 wt % TBAF. The solution of CDI/BriBA was then added slowly and left to react for 24 h at 40 °C. The final product was precipitated with ice cold ethanol, methanol or isopropanol, centrifuged, washed with alcohol (3 times), neutralized with sodium carbonate, and then lyophilized from water. The dry product was characterized by proton NMR in D₂O.

SET-LRP PISA from Alginate-Br Macroinitiator. In a typical SET-LRP reaction, 50–150 mg of alginate-Br (2 mol % BrIB) was dissolved in 5–10 mL of water. Next 500–1500 μL of MMA was added and vigorously stirred to produce a dispersion of MMA droplets in water. Methanol was then slowly added until complete dissolution of MMA resulted, yielding a homogeneous water/methanol mixture. Then 50–90 μL of Me₆Tren ligand was finally added to the solution. The monomer/initiator/ligand molar ratios were generally kept at 1000:1:20. The solution was then transferred to a 25 mL reaction tube with a resealable injection port and a vent, and subjected to three freeze–pump–thaw cycles using liquid nitrogen, vacuum pump, and warm water to remove dissolved oxygen. Copper wire (10 cm) was rolled onto a small stir bar and dropped into the degassed solution to initiate polymerization. The reaction proceeded at 25 °C. After the formation of micelles, the final solution was purged with air, diluted with water (>10), and dialyzed against 2 L of distilled water for 1–2 days while changing the dialysis solvent three times.

Characterization of Micelles. After dialysis, a solution of micelles was divided into portions for post self-assembly characterization. A small aliquot was lyophilized to determine the concentration of micelles in water to later be used for calculation of critical micelle concentration (CMC). The same solution was used for TEM imaging where morphology and the approximate size of the self-assembled structures were determined. Micelle diameter and size distributions were determined by DLS.

Analysis of PMMA Grafts. To characterize the molecular weight progression of PMMA grafts, 2 mL aliquots were withdrawn from the reaction solution 1 h before and after self-assembly, bubbled with air, and dried in a vacuum oven at 70 °C. Micelles were recovered by resuspending in water and sonicating the samples at 40 kHz and 50 °C. Samples were then heated to 80 °C and an equal amount of 50%

H_2O_2 was added to degrade the micellar shell composed of alginate. After a reaction time of 30 min, the white precipitate (PMMA) that formed was recovered by centrifugation at 3500 rpm, dissolved in acetone, passed through a 0.2 μm filter, air-dried, and redissolved in THF to a concentration of 1–2 mg/mL for GPC analysis.

Critical Micelle Concentration (CMC). Series of dilutions of the original micelle solutions were prepared, and 30 μL of C153 in THF (6.6×10^{-5} M) was added to 2 mL to each sample, followed by sonication for 10 min at 40 kHz. The fluorescence intensity of each dilution was then measured with a spectrofluorometer and plotted against $\log[\text{concentration}]$ of the amphiphilic material. Intersection of the two extrapolated linear slopes, one representing a low intensity region and another region of rapidly increasing intensity, gave the critical micelle concentration of the alginate-*graft*-copolymer in water. Light scattering intensity was also measured at the same dilutions using DLS, and CMC values were determined in a similar manner.

RESULTS AND DISCUSSION

The objective of this work was to synthesize an alginate-based amphiphilic material capable of self-assembly and with potential use as a drug carrier. The rationale behind the use of LRP as a grafting method lies in the ability to synthesize a wide range of well-defined polymers and block copolymers with highly controlled molecular weights and different functionalities. Figure 1 depicts a scheme summarizing the steps developed for the synthesis of an alginate graft copolymer and its subsequent self-assembly. First, native sodium alginate was partially depolymerized into low molecular weight fragments, then acidified to alginic acid and neutralized with TBAOH. The resultant alginate-TBA salt was soluble in dimethyl sulfoxide, which allowed anhydrous esterification of the alginate hydroxyl groups with CDI activated bromoisobutyric acid. In the last step, methyl methacrylate was grafted from the macroinitiator via SET-LRP. Continuous increase in the hydrophobicity of the extending poly(methyl methacrylate) grafts resulted in the self-assembly of amphiphilic copolymers, forming a colloidal solution with well-defined micellar structures. The details of the reaction steps are presented in the following sections.

Depolymerization. High molecular weight alginate was depolymerized into shorter fragments to be used as a hydrophilic part in the preparation of amphiphilic graft copolymers. The use of low molecular weight alginate ensures the formation of small micelles, which is preferred, to facilitate penetration of tissues as a drug delivery vesicle. Molecular weight was reduced in the presence of H_2O_2 and under high temperature to initiate H_2O_2 decomposition into radicals. Molecular weight reduction was evident from both the DLS and GPC measurements as presented in Figure 2. Measuring molecular weight based on the principles of light scattering and chromatography produced similar results, and showed that most of the degradation occurred in the first hour. According to the DLS data, alginate was degraded to 34 000 g/mol fragments in the first hour and to approximately 10 000 g/mol fragments in the remaining 2 h. GPC showed more rapid degradation from 280 000 to 20 000 g/mol in the first 30 min. Since the GPC was calibrated with poly(ethylene oxide) (PEO) standards, the calculated values are PEO-equivalent molecular weights, which may account for the difference in final molecular weight values between DLS and GPC.

Further degradation experiments produced alginate fragments of 16 000 and 23 000 g/mol, measured using aq-GPC, by slightly increasing or decreasing the amount of hydrogen peroxide. Low molecular weight fragments with molecular weight of 20 000 g/mol were chosen as a suitable size for the

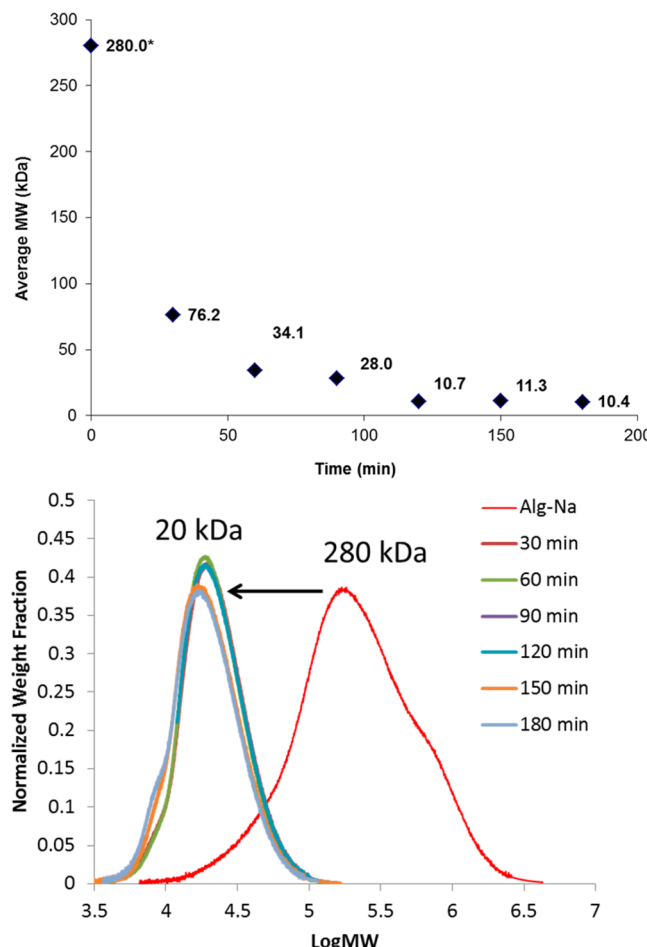


Figure 2. Molecular weight measurements by DLS (top) based on averages of three samples, and molecular weight distribution measurements by aq-GPC (bottom) of original and degraded alginate samples. *Measured with aq-GPC.

hydrophilic portion of the desired amphiphilic polymer. The rationale was to have an alginate fragment small enough to make up a small micelle, but large enough to be recovered from organic solvents in the following reactions and large enough to retain the hydrophilic character of the polymer.

Solubility Modification. Low molecular weight alginic acid was then neutralized with TBAOH to produce alginate-TBA (Alg-TBA). After lyophilization, the samples showed a doubling in mass, meaning that the alginate content is about 50% by weight. From the proton NMR spectrum shown in Figure 3, the structure of Alg-TBA was confirmed with peaks between 3.7 and 5.2 ppm representing alginate backbone hydrogens (NMR of unmodified alginate is shown in Figure S1 in the Supporting Information for comparison) and four peaks from butyl hydrogens on TBA (0.89 ppm, 3H, t; 1.30 ppm, 2H, m; 1.60 ppm, 2H, m; 3.14 ppm, 2H, m).

The solubility of Alg-TBA was then assessed in the following polar aprotic organic solvents: DMSO, DMF, and THF with and without TBAF added. It was found that 1% (w/v) Alg-TBA was highly soluble in DMSO and DMF with 1–10% TBAF, slightly soluble in pure DMSO and DMF, and insoluble in THF with or without TBAF. TBAF is thought to aid the solvation of Alg-TBA in DMF and DMSO by first providing an excess cation supply during dissolution and also by solvating attached TBA groups.

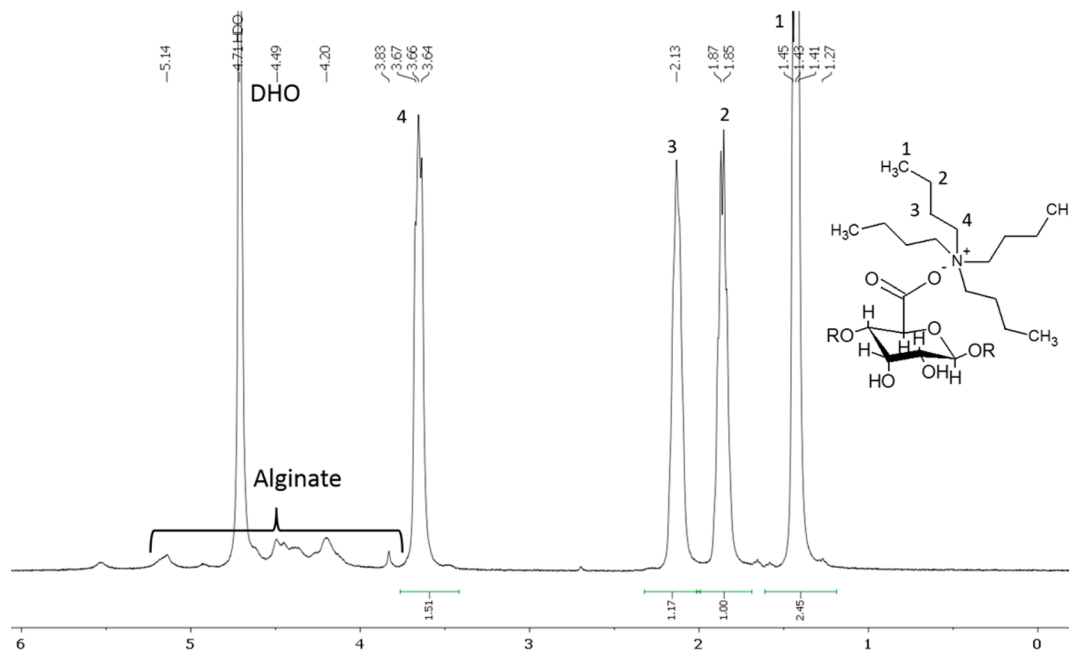


Figure 3. Proton NMR spectrum of alginate-TBA in D_2O .

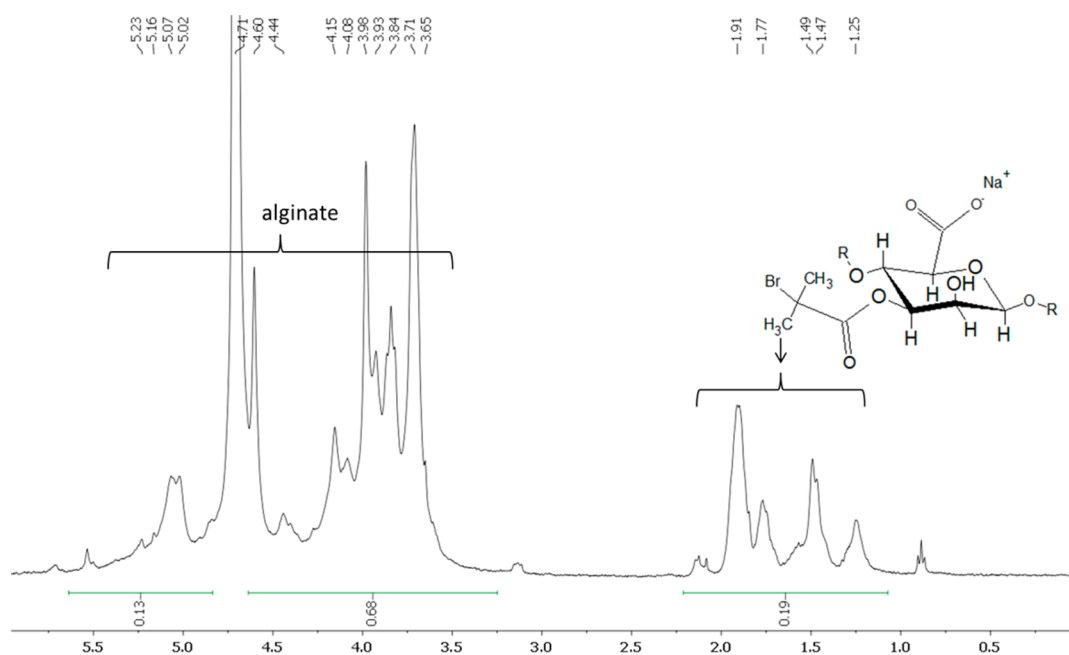


Figure 4. Proton NMR of Alg-Br macroinitiator (with DS of 0.2) in D_2O , prepared via CDI activated coupling of α -BrIBA.

Attachment of Initiator. We synthesized LRP macroinitiator with the use of BrIBA and CDI as an esterification activator. Figure 4 shows a proton NMR of alginate macroinitiator synthesized via CDI activated coupling of BrIBA. The broad singlets between 1.2 and 2.2 ppm represent methyl hydrogens from bromoisobutyryl groups. The presence of multiple signals with different chemical shifts from the bromoisobutyryl (compared to one singlet typically located at 1.8 ppm) was likely due to esterification at different locations on alginate, both on the sugar ring (two reactive hydroxyl groups) and at different regions on the alginate G/M copolymer (MM, GM/MG, and GG). These two factors resulted in the diastereotopic isobutyryl methyl groups occupying a variety of nonequivalent chemical environments,

thus producing a complex spectrum in that ppm region. Retained alginate peaks can be seen at 3.7–5.0 ppm and TBA was no longer present as it was removed during precipitation in isopropanol/dilute HCl after the reaction. The DS was calculated by integration of alginate and methyl peaks, followed by ratio correction for the number of hydrogens responsible for the integrated area (SH alginate integrated around DHO peak; 6H BrIB). The DS calculated from the spectrum in Figure 3 was 0.2 which translates to 10 initiating groups per alginate chain (see S2 in the Supporting Information for sample calculations). The macroinitiator with DS = 0.2 was synthesized with excess molar amounts of BrIBA/CDI to alginate. Macroinitiators with smaller DS (~0.02), synthesized with ~1:1:1 molar ratio of alginate/BriBA/CDI, translating to 1–2

initiating sites per alginate, were used for polymerizations to produce a graft copolymer with a more balanced amphiphilic character.

SET-LRP PISA. Growth of hydrophobic chains from the hydrophilic alginate macroinitiator resulted in PISA in the water/methanol solvent system that was initially selected to dissolve the macroinitiator and the monomer. Self-assembly could be visually observed, as the polymerization solution turned cloudy or milky white over a 1–3 h period. The onset time of PISA was defined as the time at which solution started to become turbid. The observed difference in times reported in Table 1 for the onset of turbidity was most likely due to the

Table 1. Reaction Conditions in Terms of Reagent Composition for Four Different Experiments and the Respective Onset Time of PISA

reaction	macroinitiator concentration (mg/mL)	monomer/initiator/ligand molar ratio	water/methanol ratio (v/v)	onset time of PISA (min)
1	6.2	100:0.12:2	5:3	60
2	7.5	100:0.07:2	5:4	100
3	5.5	100:0.10:3	5:4	150
4	7.5	100:0.14:2	5:3	60

differences in water to methanol ratios and the final macroinitiator concentration. This is a result of the individual adjustment of the solvent mixture for each reaction in order to cosolubilize alginate and MMA. Reactions with higher water to methanol ratios (reactions 1 and 4 from Table 1) would have earlier PISA onset times compared to those with more methanol (reactions 2 and 3). Reactions 2 and 3 with more methanol allowed longer PMMA chain growth while still being solvated in the solution before PISA. An increased amount of ligand (compared to typically low amounts used in SET-LRP (initiator/ligand 1:0.1)³⁵) was added in the reaction solution to minimize the amount of free charged copper species that could bind to alginate. The presence of PMMA within the micellar

core was confirmed by treating the dialyzed micellar solution with H₂O₂ at 80 °C. This step depolymerized the outer shell of the micelles made up of alginate. PMMA was confirmed to be stable under these conditions and not affected by H₂O₂ (see S3 in the Supporting Information). As the alginate shell degraded, the milky solution turned clear and the formation of white precipitate was visible. After recovery, the white precipitate was characterized by NMR and confirmed to be PMMA (Figure 5). Molecular weight progression of growing PMMA chains before and after self-assembly was characterized by treating time-samples with H₂O₂ at 80 °C, after evaporating the residual monomer, to completely degrade the alginate, recovering the PMMA and determining the molecular weight distributions using GPC as shown in Table 2. PMMA grafts grew to a

Table 2. Molecular Weight Data for PMMA Grafts from SET-LRP PISA^a

reaction time (min)	M _n (g/mol)	M _w (g/mol)	PDI
90	71 100	79 500	1.12
120	75 700	90 600	1.20
150	223 400	502 600	2.25
180	190 500	412 800	2.17
210	293 800	495 200	1.69
240	222 900	459 500	2.06

^aThe onset of PISA was observed to occur at 130 min.

significant chain length (~75K g/mol) before the onset of PISA was observed. Methanol and methanol/water as solvents are known to promote the disproportionation of Cu(I)X species into Cu(0) and Cu(II)X₂ complex during SET-LRP resulting in “ultrafast” polymerization.^{48,49} This could explain the formation of relatively long PMMA grafts in 90 min. The narrow polydispersity of PMMA prior to self-assembly is indicative of living polymerization. Well controlled SET-LRP prior to onset of PISA was also demonstrated by observing first-order kinetic behavior presented in Figure S4a. Linear dependence of log of monomer concentration on time means that the number of

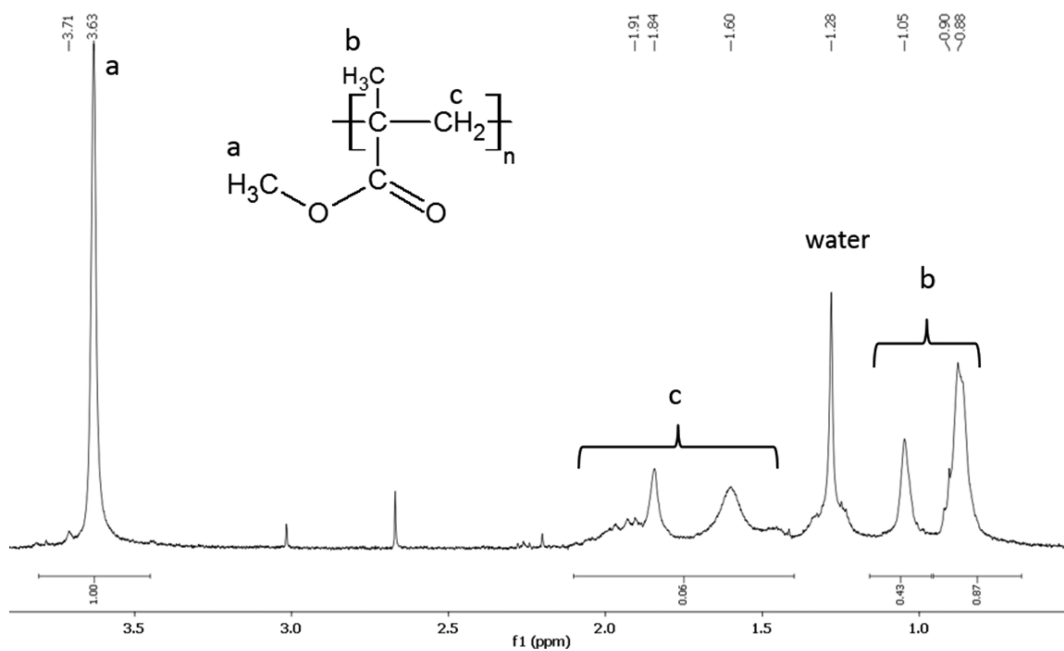


Figure 5. Proton NMR in CDCl₃ of PMMA recovered after treatment of alginate-g-pMMA micelles with H₂O₂.

active propagating species remains constant. Finally, number-average molecular weight on PMMA increased as a linear function of monomer conversion (Figure S4b), which is another confirmation of maintaining constant number of propagating chains during polymerization. After PISA, there is a dramatic jump in molecular weight and PDI of the recovered PMMA, most likely due to poorly controlled polymerization and biomolecular radical termination of living PMMA chains within the self-assembled micelles. Once the micelle forms, the monomer is capable of diffusing into the micelle core at a faster rate than the Cu/ligand complexes thus causing a disruption in SET-LRP cycle.

DLS size measurements were performed on several final micellar solutions from different experiments. The experiments had slight variation in macroinitiator concentration, monomer/initiator/ligand ratios, and the water/methanol ratio. The resultant micelle sizes were found to be between 50 and 340 nm with narrow size polydispersities (Figure 6). DLS was

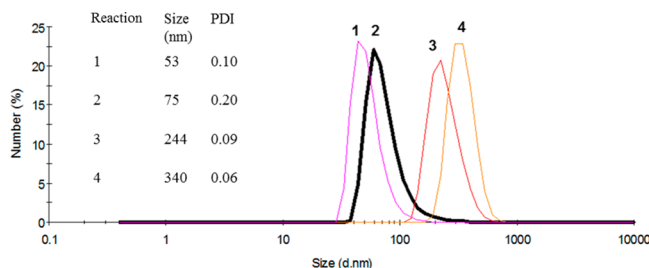


Figure 6. DLS size measurements of dialyzed micellar solutions taken from four reactions described in Table 1.

performed to monitor the progression of particle size during the reaction. From Figure 7, it can be seen that particles around

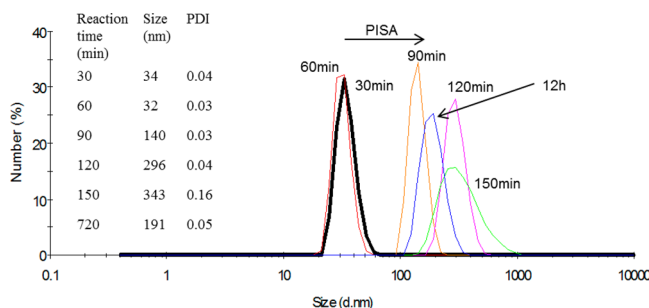


Figure 7. DLS size measurements of time samples taken directly from the polymerization reaction.

30 nm had narrow size polydispersities (0.03–0.04) prior to the observed onset of PISA. It would appear that the particles were the PMMA grafts attached to the alginate which was still freely dissolved in the water/methanol mixture. Due to the aqueous environment, growing PMMA chains may form a compact ball-like, precipitated state due to PMMA hydrophobicity, causing light scattering and identified through DLS as individual particles. These size measurements prior to the onset of PISA were in agreement with molecular weight distributions determined over time by GPC. After PISA, there was a significant increase in particle size with time, indicative of micelle formation. The measured particle diameter increased to ~300 nm over the period of 1 h after PISA and subsequently decreased over the following 12 h to ~200 nm. This change in

the size was likely due to the rearrangement of PMMA chains into more compact conformation and diffusion of any methanol and water from inside the micellar core. Micelles may be appreciably swollen with water and methanol in the early stages of the PISA process, and that the extent of swelling decreases as more PMMA is grafted, making the micelle core more hydrophobic.

Fluorescence intensity measurements of a series of dilutions of the original micellar solution, all containing the same amount of C153 fluorescent probe, showed a region of low intensity in the lower end of concentration as seen in Figure 8a. As the

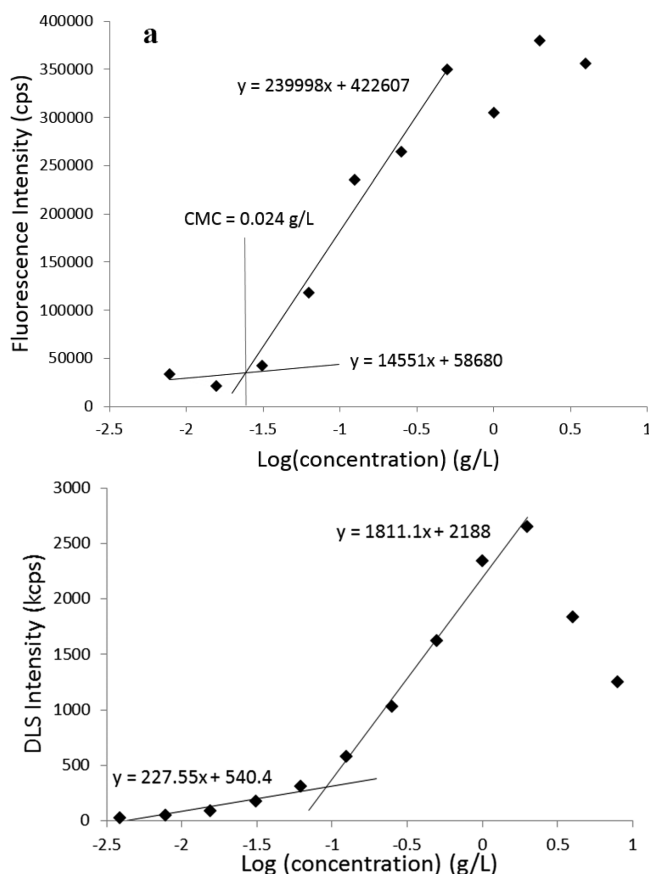


Figure 8. CMC of alginate-g-pMMA micelles determined by fluorescence (a) and DLS (b).

concentration increased, there was a rapid increase in intensity indicating that the C153 probe was leaving the aqueous phase and entering a hydrophobic environment where it has a higher solubility and therefore stronger fluorescence. This was an indication of self-assembly of alginate-*graft*-pMMA copolymers into micelles. The CMC by fluorescence was calculated to be 0.024 g/L. Light scattering intensity of the same dilutions when plotted against concentration, produced a plot (Figure 8b) similar to the fluorescence plot with a CMC of 0.091 g/L. These CMC values are within the range of published values for both polysaccharide based and fully synthetic micelles. For instance, previously synthesized alginate based amphiphilic materials self-assemble above values of CMC of 1.35 g/L⁴⁴ and 0.002–0.003 g/L⁴⁵ while more conventional surfactants such as 1,2-distearoyl-sn-glycero-3-phosphoethanolamine-polyethylene glycol-2000 have CMC values of ~0.035 g/L.⁵⁰

TEM images in Figure 9 show spherical particles resembling self-assembled micellar structures. The particle shape is

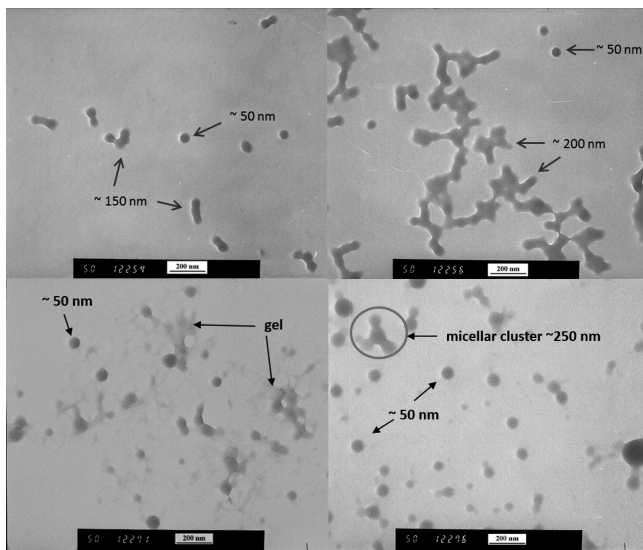


Figure 9. TEM images of alginate-g-pMMA micelles produced by SET-LRP PISA.

spherical and resembles self-assembled micellar structures. From several TEM images, it may be seen that micelles either were individually dispersed or formed small clusters (2–4 micelles) or larger aggregates. The size of the micelles observed from TEM was approximately 50–70 nm. The presence of micellar aggregates could be the result of traces of Cu(II) species that may lead to cross-linking between micellar shells. The presence of such aggregates, even in filtered, dialyzed, and sonicated samples could also explain the higher DLS size measurements noted in some experiments.

One disadvantage of using SET-LRP from alginate is the undesired interaction of charged Cu species with alginate carboxyl groups, which can result in partial gelation during the reaction. Such gelation is visible on TEM and appears as a more transparent material around micelles as may be observed in Figure 9. Poor solubility of MMA in an aqueous reaction mixture was improved by addition of methanol; however, this in turn negatively affected solubility of the alginate macro-initiator. There was a very short “window” of cosolubility adjusted with methanol to allow solubility of both alginate and MMA, and was a rather challenging step to reproduce. However, pushing the methanol content to the limit just before alginate precipitates, seemed to prolong extension of PMMA grafts before self-assembly. Therefore, the cosolvent system could be used to control the onset of self-assembly and the molecular weight of the grafted chains.

The ability to prepare micelles with alginate on the outer shell, which in the future could be further functionalized with targeted delivery ligands and drugs, and a graft copolymer core with a wide range of functionalities (drug loading and conjugation, temperature, and pH response) via LRP suggests that alginate-g-pMMA micelles have the potential to be an interesting template to be applied as “smart”, nanoscale, drug loaded vesicles with a complex and highly reproducible architecture. While continuing to explore several modifications to the amphiphilic material and resulting micelles as described in this work, we are presently testing them for the ability to encapsulate and release hydrophobic drugs and to penetrate cells. Because alginate use extends beyond biomedical materials and drug release, we suggest that alginates with well-defined,

highly controlled, and potentially versatile polymer grafts should find new and important applications.

CONCLUSIONS

Alginate graft copolymers were synthesized by SET-LRP, forming micelles during polymerization via PISA. Alginate, being a poorly modifiable polysaccharide due to its insolubility in any solvents except water, has not previously been used for grafting with living radical polymerization, whereas most other polysaccharides have been functionalized and grafted to produce novel hybrid polymers. In this paper, we have reported a synthetic route that allows grafting of synthetic polymers using LRP from alginate. This provides opportunities to synthesize new alginate-based materials with varying properties such as molecular weight of the alginate fragment, graft density, and molecular weight and composition of grafts. Micelles with alginate on the outer shell may have numerous benefits in the area of drug delivery such as vehicles for controlled release, with the potential for postpolymerization conjugation of drugs and signal molecules for targeted drug delivery and possible cross-linking of micelles to produce hybrid nanohydrogel systems.

ASSOCIATED CONTENT

S Supporting Information

S1: NMR of alginate. S2: Sample calculation of DS of alginate macroinitiator. S3: Stability of MMA in H₂O₂. Figure S3: GPC traces of PMMA before and after treatment with H₂O₂. S4: Confirmation of SET-LRP of MMA. Figure S4a: Dependence of ln([M₀]/[M]) on time prior to the onset of PISA determined by NMR. Figure S4b: Dependence of molecular weight of PMMA on conversion prior to the onset of PISA. Figure S4c: Progression of molecular weight and polydispersity of PMMA over time before and after the onset of PISA. The Supporting Information is available free of charge on the ACS Publications website at DOI: 10.1021/acs.biomac.5b00470.

AUTHOR INFORMATION

Corresponding Authors

*E-mail: neufeld@queensu.ca.
*E-mail: michael.cunningham@queensu.ca.

Notes

The authors declare no competing financial interest.

ACKNOWLEDGMENTS

Authors thank the Natural Sciences and Engineering Research Council of Canada and the Ontario Ministry of the Environment through the Council of Ontario Universities (MFC) for financial support. V.K. is the recipient of the R. Samuel McLaughlin Fellowship of the School of Graduate Studies of Queen’s University.

REFERENCES

- (1) Zhang, N.; Wardwell, P. R.; Bader, R. A. *Pharmaceutics* **2013**, *5*, 329–352.
- (2) Liu, Z.; Jiao, Y.; Wang, Y.; Zhou, C.; Zhang, Z. *Adv. Drug Delivery Rev.* **2008**, *60*, 1650–1662.
- (3) Lee, K. Y.; Mooney, D. J. *Prog. Polym. Sci.* **2012**, *37*, 106–126.
- (4) Draget, K. I.; Smidsrød, O.; Skjåk-Bræk, G. *Biopolym. Online* **2005**, DOI: 10.1002/3527600035.bpol6008.
- (5) Pawar, S. N.; Edgar, K. J. *Biomaterials* **2012**, *33*, 3279–3305.
- (6) Thu, B.; Bruheim, P.; Espenvik, T.; Smidsrød, O.; Soon-Shiong, P.; Skjåk-Bræk, G. *Biomaterials* **1996**, *17*, 1069–1079.

- (7) Draget, K. I.; Bræk, G. S.; Smidsrød, O. *Carbohydr. Polym.* **1994**, *25*, 31–38.
- (8) Skjåk-Bræk, G.; Grasdalen, H.; Smidsrød, O. *Carbohydr. Polym.* **1989**, *10*, 31–54.
- (9) Draget, K. I.; Skjåk-Bræk, G.; Smidsrød, O. *Int. J. Biol. Macromol.* **1997**, *21*, 47–55.
- (10) Smidsrød, O.; Skja, G. *Trends Biotechnol.* **1990**, *8*, 71–78.
- (11) Zhu, H.; Srivastava, R.; Brown, J. Q.; McShane, M. J. *Bioconjugate Chem.* **2005**, *16*, 1451–1458.
- (12) Srivastava, R.; Brown, J. Q.; Zhu, H.; McShane, M. J. *Macromol. Biosci.* **2005**, *5*, 717–727.
- (13) Önal, S.; Zihnioglu, F. *Artif. Cells, Blood Substitutes, Biotechnol.* **2002**, *30*, 229–237.
- (14) Ahmad, Z.; Pandey, R.; Sharma, S.; Khuller, G. K. *Indian J. Chest Dis. Allied Sci.* **2006**, *48*, 171–176.
- (15) Chan, A. W.; Neufeld, R. J. *Biomaterials* **2010**, *31*, 9040–9047.
- (16) Keshaw, H.; Forbes, A.; Day, R. M. *Biomaterials* **2005**, *26*, 4171–4179.
- (17) Kühtreiber, W. M.; Lanza, R. P.; Chick, W. L. *Cell encapsulation technology and therapeutics*; Springer Science & Business Media: Birkhäuser: Boston, 1999.
- (18) Tønnesen, H. H.; Karlsen, J. *Drug Dev. Ind. Pharm.* **2002**, *28*, 621–630.
- (19) Yang, J.-S.; Xie, Y.-J.; He, W. *Carbohydr. Polym.* **2011**, *84*, 33–39.
- (20) Augst, A. D.; Kong, H. J.; Mooney, D. J. *Macromol. Biosci.* **2006**, *6*, 623–633.
- (21) Matyjaszewski, K. Controlled/Living Radical Polymerization: State of the Art in 2005. In *Controlled Radical Polymerization: From Synthesis to Materials*; Matyjaszewski, K., Ed.; ACS Symposium Series 944; American Chemical Society: Washington, DC, 2005; Chapter 1, pp 2–12.
- (22) Percec, V.; Guliashvili, T.; Ladislaw, J. S.; Wistrand, A.; Stjerndahl, A.; Sienkowska, M. J.; Monteiro, M. J.; Sahoo, S. *J. Am. Chem. Soc.* **2006**, *128*, 14156–14165.
- (23) Matyjaszewski, K. Controlled/Living Radical Polymerization: State of the Art in 2002. In *Advances in Controlled/Living Radical Polymerization*; Matyjaszewski, K., Ed.; ACS Symposium Series 854; American Chemical Society: Washington, DC, 2003; pp 130–147.
- (24) Konkolewicz, D.; Wang, Y.; Krys, P.; Zhong, M.; Isse, A. A.; Gennaro, A.; Matyjaszewski, K. *Polym. Chem.* **2014**, *5*, 4396–4417.
- (25) Nguyen, N. H.; Rosen, B. M.; Lligadas, G.; Percec, V. *Macromolecules* **2009**, *42*, 2379–2386.
- (26) Percec, V.; Popov, A. V.; Ramirez-Castillo, E.; Monteiro, M.; Barboiu, B.; Weichold, O.; Asandei, A. D.; Mitchell, C. M. *J. Am. Chem. Soc.* **2002**, *124*, 4940–4941.
- (27) Rosen, B. M.; Percec, V. *Chem. Rev.* **2009**, *109*, 5069–5119.
- (28) Zhang, N.; Samanta, S. R.; Rosen, B. M.; Percec, V. *Chem. Rev.* **2014**, *114*, 5848–5958.
- (29) Samanta, S. R.; Sun, H.-J.; Anastasaki, A.; Haddleton, D. M.; Percec, V. *Polym. Chem.* **2014**, *5*, 89–95.
- (30) Leng, X.; Nguyen, N. H.; van Beusekom, B.; Wilson, D. A.; Percec, V. *Polym. Chem.* **2013**, *4*, 2995–3004.
- (31) Nguyen, N. H.; Rodriguez-Emmenegger, C.; Brynda, E.; Sedlakova, Z.; Percec, V. *Polym. Chem.* **2013**, *4*, 2424–2427.
- (32) Nguyen, N. H.; Kulis, J.; Sun, H.-J.; Jia, Z.; Van Beusekom, B.; Levere, M. E.; Wilson, D. A.; Monteiro, M. J.; Percec, V. *Polym. Chem.* **2013**, *4*, 144–155.
- (33) Levere, M. E.; Nguyen, N. H.; Leng, X.; Percec, V. *Polym. Chem.* **2013**, *4*, 1635–1647.
- (34) Samanta, S.; Nikolaou, V.; Keller, S.; Monteiro, M.; Wilson, D. A.; Haddleton, D.; Percec, V. Aqueous SET-LRP Catalyzed with “in Situ” Generated Cu(0) Demonstrates Surface Mediated Activation and Bimolecular Termination. *Polym. Chem.* **2015**, DOI: 10.1039/C4PY01748J.
- (35) Nguyen, N. H.; Levere, M. E.; Kulis, J.; Monteiro, M. J.; Percec, V. *Macromolecules* **2012**, *45*, 4606–4622.
- (36) Hiltunen, M. S.; Raula, J.; Maunu, S. L. *Polym. Int.* **2011**, *1370–1379*.
- (37) Voepel, J.; Edlund, U.; Albertsson, A.-C. *J. Polym. Sci., Part A: Polym. Chem.* **2011**, *49*, 2366–2372.
- (38) Voepel, J.; Edlund, U.; Albertsson, A.-C.; Percec, V. *Biomacromolecules* **2010**, *12*, 253–259.
- (39) Li, X.; Xu, A.; Xie, H.; Yu, W.; Xie, W.; Ma, X. *Carbohydr. Polym.* **2010**, *79*, 660–664.
- (40) Pawar, S. N.; Edgar, K. J. *Biomacromolecules* **2011**, *12*, 4095–4103.
- (41) Liu, G.; Qiu, Q.; Shen, W.; An, Z. *Macromolecules* **2011**, *44*, 5237–5245.
- (42) Charleux, B.; Delaittre, G.; Rieger, J.; D’Agosto, F. *Macromolecules* **2012**, *45*, 6753–6765.
- (43) Blanazs, A.; Madsen, J.; Battaglia, G.; Ryan, A. J.; Armes, S. P. *J. Am. Chem. Soc.* **2011**, *133*, 16581–16587.
- (44) Kang, H.-A.; Shin, M. S.; Yang, J.-W. *Polym. Bull.* **2002**, *47*, 429–435.
- (45) Yang, J. S.; Zhou, Q. Q.; He, W. *Carbohydr. Polym.* **2013**, *92*, 223–227.
- (46) Dey, S.; Sreenivasan, K. *Carbohydr. Polym.* **2014**, *99*, 499–507.
- (47) Yamada, Y.; Hozumi, K.; Katagiri, F.; Kikkawa, Y.; Nomizu, M. *Pept. Sci.* **2010**, *94*, 711–720.
- (48) Lligadas, G.; Percec, V. *J. Polym. Sci., Part A: Polym. Chem.* **2008**, *46*, 2745–2754.
- (49) Nguyen, N. H.; Rosen, B. M.; Jiang, X.; Fleischmann, S.; Percec, V. *J. Polym. Sci., Part A: Polym. Chem.* **2009**, *47*, 5577–5590.
- (50) Wu, H.; Zhu, L.; Torchilin, V. P. *Biomaterials* **2013**, *34*, 1213–1222.